



Effect of Different Kernel Normalization Procedures on Vibration Behaviour of Calibrated Nonlocal Integral Continuum Model of Nanobeams

Amin Anjomshoae, Behrooz Hassani*

^a Department of Mechanical Engineering, Ferdowsi University of Mashhad, Mashhad, Iran

Abstract

Although the nonlocal integral (NI) model circumvents the inconsistencies associated with the differential model, it is shown in the present study that the way its nonlocal kernel function is normalized noticeably affects the dynamic response of nanobeams. To this aim, a two-phase nonlocal integral nanobeam model with different boundary conditions and kernel functions is considered and its natural frequencies are obtained using the Rayleigh-Ritz method. Also, the kernel function is normalized via two procedures to see the influence of each one on the vibration characteristics of nanobeam. From the results it is found that kernel normalization has a significant effect on vibration response of nanobeam and therefore must be taken into account. Further, it is found that the results from each normalized model are noticeably different from the other. Furthermore, by comparing the results of continuum NI models with those from atomistic models, it is revealed that for certain normalization schemes a calibrated nonlocal parameter cannot be found due to twofold hardening-softening behavior. Moreover, the effect of kernel type, boundary conditions and mode number is thoroughly studied. The results from current study can shed light on the way of choosing or developing more reliable equivalent continuum NI models for nanostructures.

Keywords: Nonlocal integral model; Nanobeam; Vibration Analysis; Kernel function normalization; Calibration process; Atomistic modelling.

1. Introduction

Due to superior mechanical, electrical, thermal and chemical properties, the nanostructures are being used in different nano-devices as sensors [1{Johnson, 2010 #452}], superconductors [2], supercapacitors [3] and composite reinforcements [4-6]. For instance, in composite materials, it is reported by Rafiee et al. [4] that the Young modulus and ultimate tensile strength of epoxy increase about %30 and %22, respectively, when the graphene nano-ribbons (GNRs) are used as filler. This is due to the large interface area between the GNRs and the matrix which enhances the load transfer efficiency at the interfacial region. Moreover, due to the large contact surface, GNR based sensors show higher tendency to chemical reaction, in comparison to the carbon nanotubes (CNTs), and therefore are more sensitive and precise sensors. For example, Johnson et al. [7] reported that in gas sensing, the GNR based sensor

* Corresponding author.

E-mail address: b_hassani@um.ac.ir

exhibits higher sensitivity than the CNT based sensors due to the larger specific area and better functionalization.

Based on the above applications, and more, in-depth study of these precious tiny structures is necessary to precisely predict their behaviour in different problems. There are several ways to conduct a research about mechanical behaviour of nanostructures which are mainly categorized into three groups namely experimental measurements, atomistic simulations based on semi-empirical models and theoretical studies based on modified equivalent continuum theories. Needless to say that the first method is the most realistic and reliable one. However, when dealing with a structure of very small size as nano, there could be severe limitations on tools for manipulating and repetition the same experiment. These shortcomings make the experimental studies more difficult, time consuming and expensive compared to other methods. Especially when the object of the study includes design or optimization of a typical nanodevice.

Semi empirical methods such as molecular dynamics (MD) [8] or density functional theory (DFT) [9] are the second choice for studying nanostructures. These methods use data which are previously obtained from experiment and use physical formula such as Newton's second law to predict the motion of a number of bonded atoms. Although these methods are able to produce results in agreement with experiment, they need huge computational capacities and are only applicable to relatively small nanostructures with limited number of atoms and bonds. Due to the shortcomings of experimental studies and atomistic simulations, modified continuum modelling has been vastly attended recently for predicting the behaviour of nanostructures [10-25]. The simplicity and small required computational cost enable the modified continuum modelling to be considered as an inexpensive method for design and optimization of relatively large nanostructures even in multi-physics problems. However, the key point in modified continuum modelling of nanostructures is the precise capturing of small scale effects which alter the physical properties of materials at nano scale. Most of these effects arise due to discreteness and long range cohesive forces between non-adjacent or nonlocal atoms. In this regard, one of the theories that can simply and efficiently capture these effects is the nonlocal continuum theory introduced by Eringen [10, 11] which has been claimed to be able to produce results in agreement with lattice dynamics and experimental measurements. By introducing only one scale parameter, Eringen's nonlocal theory has become one of the efficient and easy to implement theories for studying different problems including bending, vibration and buckling of beam-like [12-15], plate-like [16-20] and shell-like [21, 22] nanostructures.

It has to be noted that the nonlocal constitutive equation was originally introduced in an integral form which, by taking some mathematical assumptions (specific kernel type), can be transformed to a simplified differential form [10]. Due to its simple form, the differential form of nonlocal constitutive equation has received huge attention from the research communities [12-17, 19-26]. All of these studies claimed that the continuum model of nanostructures based on the nonlocal theory shows softer behaviour in comparison to the classical continuum theory. Although nonlocal differential form is computationally efficient, but, it has been reported that it shows inconsistency and paradox in some cases [27-33]. In fact, it was revealed that the intensity of nonlocal effect exerted on the model based on nonlocal differential form depends severely on the type of boundary and loading conditions which in some cases seems unexpected. For instance, in bending problem of a clamped-clamped nanobeam under uniform loading, there is no sign of small scale when the differential form of nonlocal elasticity theory is employed [25]. Another challenging paradox arises when the nonlocal differential form is employed to study the behaviour of a cantilever nanobeam. It was seen that the nanobeam with such boundary conditions shows stiffening behaviour which is in absolute contrast to other types of boundary conditions e.g. simply-supported [27-29]. These inconsistencies, and more, have been reported in detail by some researchers [27, 28, 32]. Due to these inconsistencies and unexpected results, the original integral form of nonlocal elasticity theory has received more attention again.

In the case of nonlocal integral (NI) modelling, Fernandez-Saez et al. [27] studied the bending problem of an Euler-Bernoulli nanobeam with different boundary and loading conditions using a mixed analytical and numerical method. They compared their results with those from differential form and reported noticeable differences between these two forms. They also announced the resolution of paradoxes arisen for cantilever and clamped nanobeams when the nonlocal integral form is employed. In another study, Tuna and Kirca [29] reported the solutions for bending of Euler-Bernoulli and Timoshenko nanobeams under various loading and boundary conditions. By changing the type of governing equation from Fredholm integral equation to Volterra integral equation and then solving it by Laplace transform, they obtained the deflections for various types of nanobeam. They also studied the vibration and buckling of Euler-Bernoulli nanobeam using the same solution procedure and reported the natural frequencies and critical loads for different nanobeam systems [30]. The inconsistencies associated with the nonlocal differential form in dynamic problem, for some boundary conditions, are claimed to be solved when the NI model is

employed. Wang et al. [31] also reported the exact closed form solutions for deflection of nanobeams under different loading and boundary conditions using two-phase nonlocal integral (TPNI) model. The vibration of nanobeam based on TPNI model was also studied by Fernández-Sáez, and Zaera [32] via transformation of integral equation to a differential one. Zhu et al. [33] also presented solutions for buckling loads of TPNI nanobeam through a solution procedure similar to that of Fernández-Sáez and Zaera. Using the finite element method, Eptaimeros et al. [34, 35] reported the dynamic response of embedded nonlocal nanobeam based on TPNI constitutive equation.

An important point while using the NI model is to ensure that the kernel function is properly normalized. It was shown in the previous authors' work [36] that, for bounded domains, the kernel function must be normalized to avoid violation of natural boundary conditions. Besides, the normalization process avoids excessive softening presented by un-normalized classical kernels. The authors also showed that the way through which the kernel function is normalized, severely changes the response of nanobeam and the obtained results. Moreover, they showed for the first time in bending case that, the results from one of the normalization schemes either cannot be matched with those from atomistic models or may lead to two different values for calibrated nonlocal parameter. Similar to bending problem, prediction of dynamic characteristics of normalized NI model of nanobeam is also an important issue which is addressed in the present work.

Another important step in developing equivalent nonlocal continuum models for nanostructures is the calibration process. In this process, the results from equivalent NI continuum model are matched with those from a corresponding atomistic model with the same size and then the associated calibrated nonlocal parameter is derived [20, 37]. The atomistic models can be a lattice structure as Eringen stated [10] which consider atoms as lumped masses and bonds as springs, or a Molecular Dynamics model [32, 37] which uses potential fields and Newton's second law, or an structural mechanics model which considers atoms as concentrated masses and bonds as structural beam elements [38]. By calibrating the nonlocal continuum model, one can not only predict the response of the nanostructure more precisely, but can also find out whether the developed nonlocal continuum model is reliable for the problem in hand or not. This, and more, was thoroughly reported and discussed in the authors' previous paper for bending problem [36].

It has to be mentioned that exact solution for governing equations based on nonlocal integral form is only available for elementary problems, e.g. one dimensional problems, and for specific kernels (exponential function). For more general or complex problems, finding an exact solutions could be very cumbersome or even impossible [31-33]. On the other hand, applying some numerical techniques such as finite element method requires special considerations for selecting nonlocal elements in neighbourhood and then assembling them to obtain global nonlocal stiffness matrices. Consequently, an efficient and simple to use meshless solution procedure such as Rayleigh-Ritz method without such limitations may always be appreciated.

In the present study, vibration behaviour of modified normalized NI continuum model of a nanobeam is thoroughly examined to see the influence of different kernel normalization procedures. To this aim, Euler-Bernoulli model of nanobeam is developed based on two-phase form of nonlocal integral constitutive equation. Total potential function of system is obtained and then is minimized to find the natural frequencies of the system using the Rayleigh-Ritz solution procedure. Since the kernel function plays an important role in NI modelling, different distributions for this function are also considered to investigate the influence of kernel type on the results. The NI model is then calibrated based on two atomistic models to find associated nonlocal parameters. Moreover, the effect of size, boundary condition and mode number is studied in detail. The calibration process is also done for different mode numbers, boundary conditions, sizes and normalization schemes for the first time.

2. Formulation

The displacement fields for the nanobeam's particles, shown in Fig. 1, are defined using the Euler-Bernoulli beam theory (EBT) as

$$u = u_0(x,t) - zw_{,x}, \quad v = v_0 = 0, \quad w = w_0 = w(x,t) \quad (1)$$

Here, u , v and w denote the displacement of an arbitrary point in x , y and z direction, respectively and u_0 , v_0 and w_0 are displacements of points located on the neutral plane. Using Eq. (1), the strains are obtained as

$$\varepsilon_{xx} = u_{0,x} - zW_{,xx}, \quad \varepsilon_{yy} = \varepsilon_{zz} = \varepsilon_{xy} = \varepsilon_{xz} = \varepsilon_{yz} = 0 \quad (2)$$

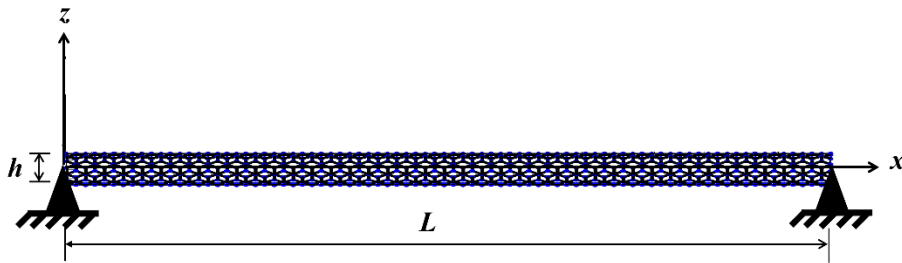


Fig 1 : Schematic of the nanobeam under study.

The constitutive equation according to the TPNI form is defined as [10, 11, 39]

$$\sigma_{ij}^{nl}(x) = \xi_1 \sigma_{ij}^l(x) + \xi_2 \int_V \alpha(|x - x'|, \tau) \sigma_{ij}^l(x') dV' \quad (3)$$

Here, σ_{ij}^{nl} and σ_{ij}^l are the nonlocal and local (classical) stress tensors, respectively. The above equation is called “Two-Phase” since it considers both the macro-scaled classical constitutive equation and nano-scaled nonlocal constitutive equation simultaneously. The parameters ξ_1 and ξ_2 are positive phase indicators with the relation $\xi_1 + \xi_2 = 1$. It is obvious that for $\xi_1 = 1$, Eq. (3) gives the classical constitutive equation and for $\xi_1 = 0$ it yields the pure nonlocal integral (PNI) constitutive equation. In Eq. (3), α is the nonlocal kernel function, which puts a weight on the strains at nonlocal or non-adjacent atoms. Similar to interatomic forces it depends on the distance between nonlocal atoms at x' and reference atom at x . The maximum value for the kernel function occurs at the local or reference point x and, similar to the interatomic forces, rapidly decays by distance. The kernel function also depends on a scale parameter $\tau = e_0 l_i / l_e$ which represents the discreteness and intensity of small scale effects. As it is seen, this parameter depends on an internal characteristic length l_i which can be bond length, granular distance or lattice parameter, and an external characteristic length l_e which can be one of sample's dimensions, crack length or wave length, and a constant e_0 which adjusts the intensity of both small scale effect and discreteness at the same time. The parameter e_0 needs to be determined for each material independently by matching results from the nonlocal model with those from atomistic models or experimental data [11, 22]. The process is referred to as “Calibration”. Some well-known one dimensional kernel functions together with their associated mathematical formulation are listed in Table 1.

According to the nonlocal continuum theory, the kernel function must satisfy the following conditions [10, 11]

$$\int_V \alpha(|x - x'|, \tau) dV' = 1 \quad (4)$$

and

$$\lim_{\tau \rightarrow 0} \alpha(|x - x'|, \tau) = \delta(|x - x'|) \quad (5)$$

The first property requires the kernel function to be normalized at each point of the body like x over the whole domain. The second property necessitates the kernel function to be a Dirac delta sequence. The first property introduces the nonlocal operator as an averaging operator by satisfying that the sum of weights on strains in all nonlocal points should be equal to unity. Further, it ensures that a uniform strain field is always resulted from a uniform stress field. The latter property, Eq. (5), also makes sure that results from nonlocal theory converge to those from classical continuum theory when the scale parameter approaches zero or the small scale effects vanish.

For a Hookean solid Eq. (3) can be rewritten as

$$\sigma_{ij}^{nl}(x) = \xi_1 S_{ijkl} \varepsilon_{kl} + \xi_2 \int_V \alpha(|x - x'|, \tau) S_{ijkl} \varepsilon_{kl}(x') dV' \quad (6)$$

In which, S_{ijkl} is the fourth-order elasticity tensor.

Table 1: One dimensional kernel functions and their associated mathematical expressions.

Kernel type	Mathematical expression
Exponential	$\alpha(x-x' , \tau) = \frac{1}{2\tau} \exp\left(\frac{ x-x' }{\tau}\right)$
Gaussian	$\alpha(x-x' , \tau) = \frac{1}{\sqrt{\pi}\tau} \exp\left(-\frac{(x-x')^2}{\tau^2}\right)$
Modified Bessel	$\alpha(x-x' , \tau) = \frac{1}{\pi\tau} K_0\left(\frac{\sqrt{(x-x')(x-x')}}{\tau}\right)$
Triangular	$\alpha(x-x' , \tau) = \begin{cases} \frac{1}{\tau} \left(1 - \frac{ x-x' }{\tau}\right), & x-x' \leq \tau \\ 0, & x-x' > \tau \end{cases}$

Substituting Eq. (2) into (6) yields

$$\sigma_{xx}^{nl}(x) = -E \left(\xi_1 z w_{,xx} + \xi_2 \int_{V'} \alpha(|x-x'|, \tau) z' w_{,x'x'} dV' \right) \tag{7}$$

In which, E is the Young's modulus of nanobeam and $w_{,xx}$ denotes the curvature.

Using stress field in Eq. (7), the moment and shear resultants are respectively obtained as

$$M^{nl}(x) = \int_A z \sigma_{xx}^{nl}(x) dA = EI \left(\xi_1 w_{,xx} + \xi_2 \int_0^L \alpha(|x-x'|, \tau) w_{,x'x'} dx' \right) \tag{8}$$

and

$$Q^{nl}(x) = -M_{,x}^{nl} = -EI \left(\xi_1 w_{,xxx} + \xi_2 \int_0^L \alpha(|x-x'|, \tau) w_{,x'x'} dx' \right)_{,x} \tag{9}$$

Here, EI denotes the bending stiffness of nanobeam. The total potential energy of the nanobeam is defined by

$$\Pi = U + T \tag{10}$$

in which, U is the total stored elastic energy in the nanobeam defined as

$$U = \frac{EI}{2} \left[\xi_1 \int_0^L (w_{,xx})^2 dx + \xi_2 \int_0^L \int_0^L \alpha(|x-x'|, \tau) w_{,xx} w_{,x'x'} dx' dx \right] \tag{11}$$

and T is the kinetic energy of nanobeam which is obtained as

$$T = \int_0^L \left[m_0 (\dot{w})^2 + m_2 (\dot{w}_{,x})^2 \right] dx \tag{12}$$

Here, m_0 and m_2 are, respectively, the first and second moment of inertia of nanobeam defined as

$$m_0 = \int_A \rho dA \tag{13a}$$

$$m_2 = \int_A z^2 \rho dA \tag{13b}$$

In above relations, ρ and A are the density and cross-section area of nanobeam, respectively. The dot over the parameters also means derivation with respect to time.

Substituting Eqs. (11) and (12) into (10), and using displacement fields in Eq. (1), the total potential energy for the nanobeam is obtained as

$$\Pi = \frac{1}{2} \left[\xi_1 \int_0^L (w_{,xx})^2 dx + \xi_2 \int_0^L \int_0^L \alpha(|x-x'|, \tau) w_{,xx} w_{,x'x'} dx' dx \right] + \frac{1}{2} \int_0^L \left[m_0 (\dot{w})^2 + m_2 (\dot{w}_{,x})^2 \right] dx \quad (14)$$

Putting the Dirac delta function as the kernel function in the above equation, total potential energy for classical continuum body (EBT beam) will be obtained. Assuming harmonic motion as $w(x,t)=W(x)\exp(i\omega t)$ the time independent expression for the total potential energy is obtained as

$$\Pi = \frac{EI}{2} \left[\xi_1 \int_0^L (W_{,xx})^2 dx + \xi_2 \int_0^L \int_0^L \alpha(|x-x'|, \tau) W_{,xx} W_{,x'x'} dx' dx \right] - \frac{\omega^2}{2} \int_0^L \left[m_0 (W)^2 + m_2 (W_{,x})^2 \right] dx \quad (15)$$

Here, $W(x)$ is the deflection function of neutral axis and ω is the circular frequency of nanobeam.

As mentioned before, the nonlocal kernel function must satisfy the normalization condition in Eq. (4) in all points of the medium. For classical kernels however, this condition is not satisfied for the points at or near boundaries of bounded domains due to truncation of the kernel function as shown in Fig. 2. In this situation the classical kernels shouldn't be used otherwise the natural boundary conditions may fail to be satisfied [36]. To overcome this, few normalization procedures have been introduced by researchers for the fracture and plasticity analysis of the structures based on the nonlocal continuum theory [40, 41]. These procedures have been less attended in the study of nanostructures based on nonlocal integral models.

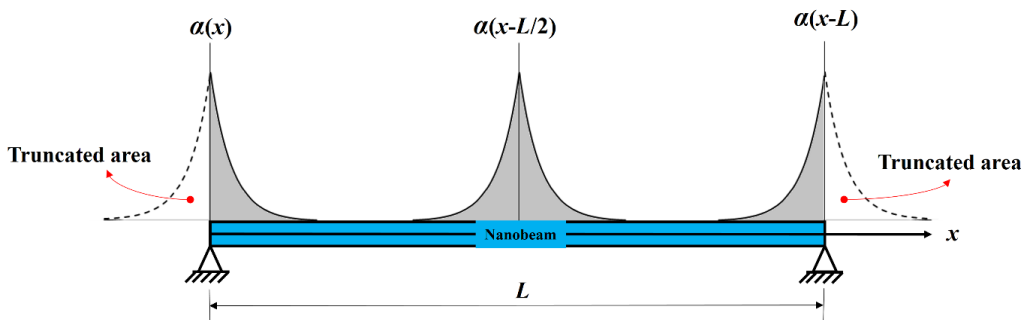


Fig 2 : Truncation of the kernel function at the boundaries for bounded nanostructures.

Among normalization schemes, the following two approaches have been employed the most [11, 40, 41]

$$\alpha_{\text{mod}}(\mathbf{x}, \mathbf{x}', \tau) = \left[1 - \int_{\mathbf{V}} \alpha(\mathbf{x}, \mathbf{X}, \tau) dV_{\mathbf{X}} \right] \delta(\mathbf{x}, \mathbf{x}') + \alpha(\mathbf{x}, \mathbf{x}', \tau) \quad (16)$$

and

$$\alpha_{\text{mod}}(\mathbf{x}, \mathbf{x}', \tau) = \frac{\alpha(\mathbf{x}, \mathbf{x}', \tau)}{\int_{\mathbf{V}} \alpha(\mathbf{x}, \mathbf{X}, \tau) dV_{\mathbf{X}}} \quad (17)$$

Here, $\alpha(\mathbf{x}, \mathbf{x}', \tau)$ is the classical or un-normalized kernel function and can be any of the functions in Table 1.

The modified kernel α_{mod} in both equations satisfies the conditions in Eq. (4) and (5) for all points of the nanobeam. Following the names used in [36], here the first scheme in Eq. (16) is referred to as “Additive normalization” and the second scheme in Eq. (17) is called “Fractional normalization” scheme, respectively.

Eringen [11] used the Fractional normalization scheme to determine the stress fields for a semi-finite elastic body under rigid stamping. Eptaimeros et al. [34, 35] employed the Additive scheme for dynamic analysis of nanobeams

based on TPNI constitutive equation. However, as it will be shown in the present study, the Additive scheme shows unexpected two-fold softening-hardening behaviour which leads to severe limitation in the calibration process.

3. Solution procedure

The Rayleigh-Ritz (RR) method is adopted in the present study since it was seen to be computationally efficient, fast convergent and able to deal with complicated normalized kernels [36]. According to this method, the displacement field is approximated using suitable trial functions and then the potential energy functional of the system is minimized with respect to the unknown coefficients. There are different types of trial functions however they better to be orthogonal to each other and satisfy the essential boundary conditions. Here, the polynomial trial functions are adopted. In this way, the transverse displacement of the nanobeam is defined as

$$W(x) = \sum_{i=1}^{p+1} c_i \varphi_i(x) \quad (18)$$

in which, c_i , $\varphi_i(x)$ and p denote unknown coefficients, the trial functions and the degree of polynomial set, respectively. The orthogonal trial functions are generated according to the Gram-Schmidt process as follow [42]

$$\psi_1 = \theta_1 \quad (19a)$$

$$\psi_k = \theta_k - \sum_{j=1}^{k-1} \beta_{kj} \psi_j \quad (19b)$$

in which,

$$\theta_k = x^r (L-x)^s x^{k-1} \quad (20)$$

where, r and s determine the type of edge constraint by taking 0, 1 or 2 for free, simply-supported and clamped edges, respectively. Also, β_{kj} are defined as

$$\beta_{kj} = \frac{\langle \theta_k, \psi_j \rangle}{\langle \psi_j, \psi_j \rangle} \quad (21)$$

where,

$$\langle \psi_i, \psi_j \rangle = \int_0^L \psi_i \psi_j dx \quad (22)$$

Finally, the orthogonal trial functions are obtained as

$$\varphi_i = \frac{\psi_i}{\|\psi_i\|} \quad (23)$$

in which, the norm of the function is defined as

$$\|\psi_i\| = \sqrt{\int_0^L \psi_i^2 dx} \quad (24)$$

Substituting Eq. (18) into total potential energy functional in Eq. (15) gives

$$\begin{aligned} \Pi = & \frac{EI}{2} \left[\xi_1 \int_0^L \left(\sum_{i=1}^{p+1} c_i \varphi_{i,xx} \right)^2 dx + \xi_2 \int_0^L \int_0^L \alpha(|x-x'|, \tau) \sum_{i=1}^{p+1} \sum_{j=1}^{p+1} c_i c_j \varphi_{i,xx} \varphi_{j,xx'} dx dx' \right] \\ & - \frac{\omega^2}{2} \int_0^L \left[m_0 \left(\sum_{i=1}^{p+1} c_i \varphi_i \right)^2 + m_2 \left(\sum_{i=1}^{p+1} c_i \varphi_{i,x} \right)^2 \right] dx \end{aligned} \quad (25)$$

Minimizing the above expression with respect to the unknowns c_i yields

$$([\mathbf{K}] - \omega^2[\mathbf{M}])\{\mathbf{C}\} = 0 \quad (26)$$

Here, $[\mathbf{K}]$ is the stiffness matrix with the components being as

$$K_{ij} = EI \left[\xi_1 \int_0^L \varphi_{i,xx} \varphi_{j,xx} dx + \xi_2 \int_0^L \int_0^L \alpha(|x-x'|, \tau) \varphi_{j,xx} \varphi_{i,xx'} dx dx' \right] \quad (27)$$

The vector \mathbf{C} in Eq. (26) includes the unknown coefficients and is defined as below

$$\{\mathbf{C}\} = \{c_1, c_2, \dots, c_j\}^T \quad (28)$$

The components of mass matrix, $[\mathbf{M}]$, are also given as

$$M_{ij} = m_0 \int_0^L \varphi_i \varphi_j dx + m_2 \int_0^L \varphi_{i,x} \varphi_{j,x} dx \quad (29)$$

Eq. (26) is an eigenvalue problem which can be solved for natural frequencies. The associated vector \mathbf{C} represents the eigenvector.

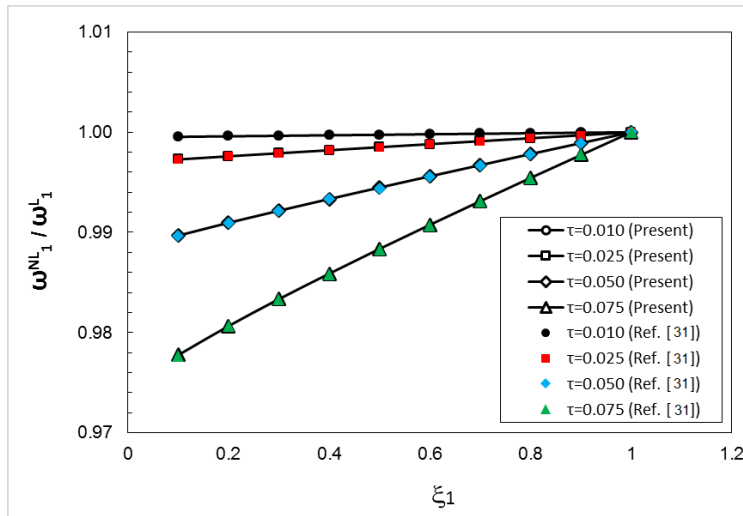
It has to be mentioned that due to distribution of normalized kernel functions, the integration rule employed here is crucial to achieve fast convergent and reliable results. In fact, for small nonlocal parameters, the kernel function becomes sharper and looks like Dirac delta function, therefore, the numerical integration techniques such as Gauss-quadrature requires a large number of Gauss points to converge. On the other hand, the Gauss technique is very efficient for higher values of nonlocal parameter for which the kernel function is smooth. Accordingly, in order to reduce the computational time, here, a combination of Gauss and Simpson integration rules is utilized for small nonlocal parameters and for large values of nonlocal parameter, the Gauss quadrature technique is employed.

4. Results and discussions

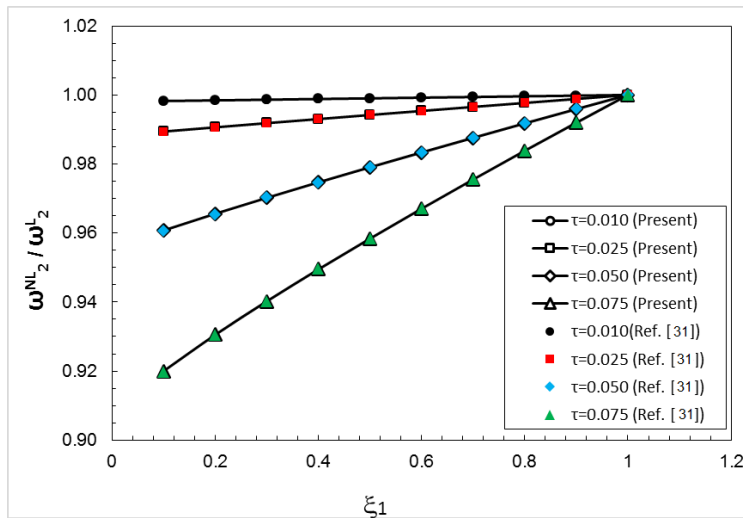
4.1. Convergence and validation studies

For convergence and validation study, the first three natural frequencies of a simply-supported NI model of nanobeam with classical un-normalized exponential kernel are calculated from Eq. (26) for $p=8$ and the results are depicted in Fig. 3 for different phase parameters ξ_1 and nonlocal parameters τ . It is seen that for a polynomial of degree 8 and higher, the results are convergent. From Fig. 3 it is found that the results obtained from current RR solution method are in good agreement with those obtained by Fernandez et al. [32]. Here and afterwards, the internal characteristic length is assumed to be constant, $l_i=a$, and the external characteristic length l_e is taken as the length of the nanobeam L . Also, the results are reported as ratios of nonlocal values with superscript "NL" to local ones with superscript "L". For better understanding, the results are also provided based on the following non-dimensional parameters.

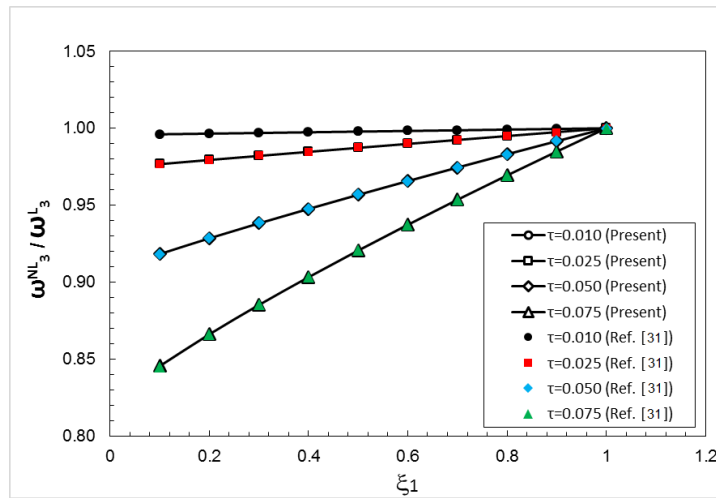
$$\bar{\omega} = \omega L^2 \sqrt{\frac{m_0}{EI}}, \quad \tau = \frac{e_0 a}{L} \quad (30)$$



(a)



(b)



(c)

Fig 3 : Validation of present solution in vibration problem for simply-supported nanobeam: (a) First vibration mode; (b) Second vibration mode; (c) Third vibration mode.

It is also found from Fig. 3 that as the phase parameter ζ_1 increases, the ratio of nonlocal frequency to local frequency increases and finally converges to 1. In fact, by increasing ζ_1 , the portion of classical part of constitutive equation in Eq. (3) increases and, correspondingly, the portion of nonlocal part, and the softening effect, decreases due to the relation $\zeta_1 + \zeta_2 = 1$.

4.2. Effect of kernel normalization procedure

To show the influence of kernel normalization procedure in more details, the frequency ratios for additively normalized nonlocal integral (ANNI) model, fractionally normalized nonlocal integral (FNNI) model and un-normalized nonlocal integral (UNNI) model of SS nanobeam are plotted against the nonlocal parameter in Fig. 4. It is seen in this figure that the frequency ratios of UNNI model are lower than those of ANNI and FNNI models, meaning that the kernel normalization procedure decreases the intensity of nonlocal softening effect. Further, it is seen in this figure that as the nonlocal parameter increases, the difference between un-normalized and normalized models increases. The maximum error percent due neglecting normalization procedure is found about %44 and %30 for Additive and Fractional normalization schemes, respectively. This implies that the effect of kernel normalization process becomes more prominent for higher nonlocal parameters and should be taken for nanostructures with severe small scale effects.

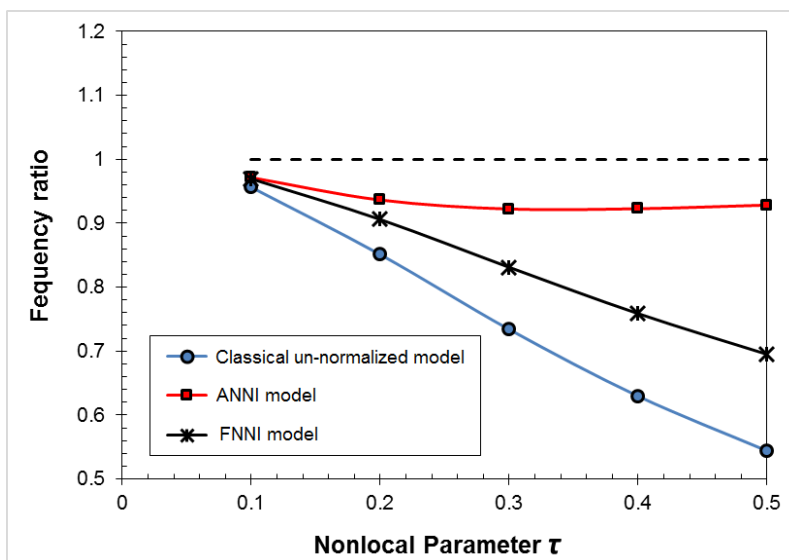


Fig 4 : Effect of different kernel normalization schemes on frequency ratio of NI nanobeam model.

By analysing the results obtained from these two normalized models, it is found that one of these models has a specific trend as the nonlocal parameter changes. To clearly show this phenomenon, the frequency ratios of ANNI model of nanobeam are plotted in Fig. 5 for a wider range of nonlocal parameter. It is seen in this figure that for small values of nonlocal parameter, the ANNI model shows a softening behaviour and then by increasing the value of nonlocal parameter this behaviour suddenly changes to a stiffening one. By further increasing the nonlocal parameter the intensity of stiffening effect decreases and the results gradually converge to the results from classical continuum theory (frequency ratio=1). This behaviour is surprising since it was expected that as the nonlocal parameter increases, the softening nonlocal effect escalates as well. But this isn't happening here. In fact, for small nonlocal parameters the kernel α is very sharp and resembles Dirac delta function. As the nonlocal parameter increases the kernel span becomes large while its maximum value, which happens at the reference point x , decreases. By further increasing the nonlocal parameter this value approaches zero and thus the first term in Eq. (16) intensifies. This causes the kernel function takes the form of Dirac delta function again and the ANNI model behaves like a classical continuum model for very large nonlocal parameters. The FNNI model, on the other hand, is seen to always show a monotonic softening behaviour as the nonlocal parameter increases. So, it is concluded that each normalization scheme predicts a significantly different behaviour for the nanobeam depending on the value of nonlocal parameter.

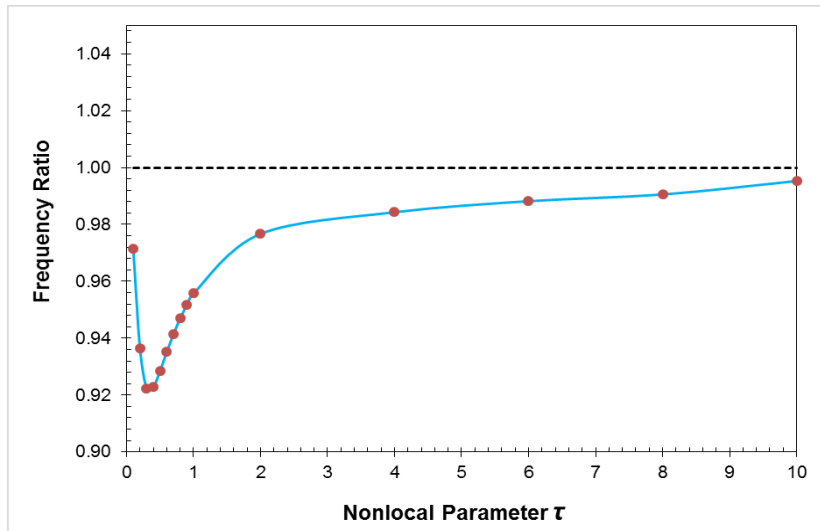


Fig 5 : Twofold softening-hardening behaviour of ANNI model in vibration problem.

4.3. Effect of nonlocal parameter and size

In this section, effect of nonlocal parameter and size is investigated in detail for FNNI model of nanobeam. The non-dimensional frequency parameter for SS nanobeam is derived for different values of lengths and nonlocal parameter and the results are shown in Fig. 6. It is seen in this figure that for a specific nonlocal parameter (e_0a), as the length of nanobeam increases the frequency parameter increases meaning that the softening nonlocal effect decreases. In fact, for a constant nonlocal parameter (e_0a), by increasing the length of the nanobeam, as an external characteristic length, the small scale parameter τ decreases and the kernel function tends to Dirac delta function. In this way, the NI model tends towards classical continuum model and therefore the natural frequencies increase and converge to classical ones.

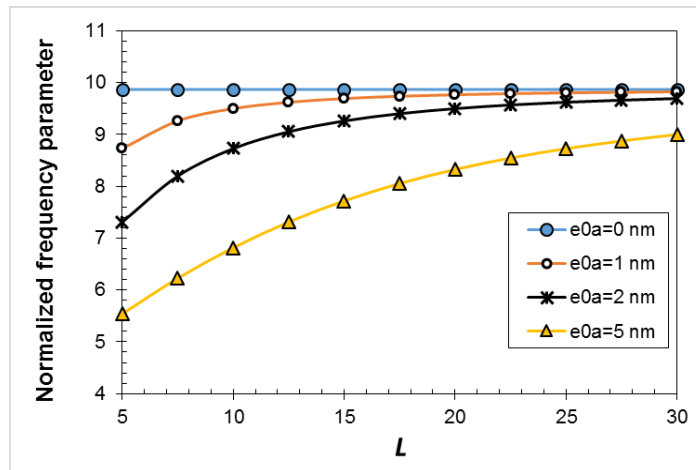


Fig 6 : Effect of size and nonlocal parameter on vibration response of FNNI model of nanobeam ($\xi_1=0.1$).

4.4. Nonlocal Effect in higher vibration modes

The nonlocal effect in higher vibration modes for normalized NI nanobeam model is also investigated and illustrated by Fig. 7. The results in this figure are the frequency ratios obtained from Eq. (26) for the first three vibration modes. It is seen in this figure that the frequency ratio decreases by the nonlocal parameter in all vibration modes denoting the softening nonlocal effect in higher modes. However, this reduction becomes more noticeable as the mode number increases translating the greater impact of nonlocal effect on higher modes. In fact, since the

nonlocal stress is dependent on the value of strain in all local and nonlocal points, and the strain for a nanobeam is dependent on its curvature, as the curvature of nanobeam varies more along its axis, the nonlocal effect is expected to intensify and increase. Since the deflection pattern of a vibrating nanobeam in higher modes has more fluctuations and variation in curvature, the nonlocal effect becomes more prominent for them. Thus, it is concluded that the nonlocal theory should be employed for nanostructures vibrating with high frequencies.

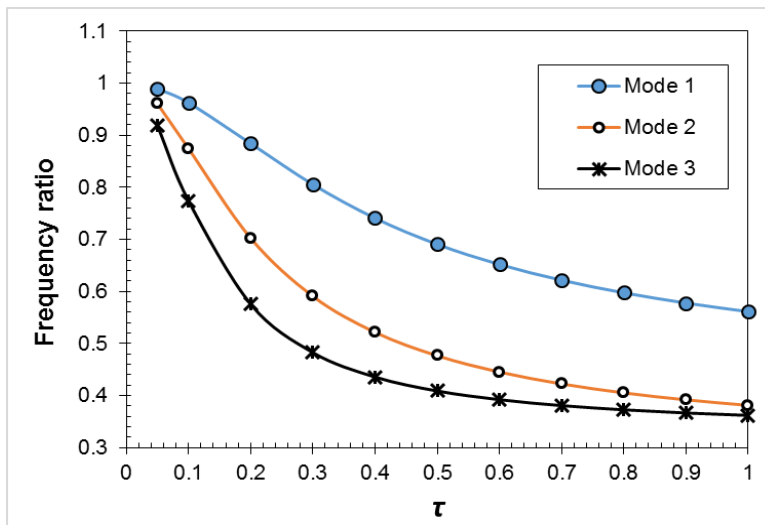


Fig 7 : Nonlocal effect in higher vibration modes.

4.5. Effect of boundary conditions

The influence of edge condition on the intensity of nonlocal effect has been vastly reported for nonlocal differential models [12, 16, 23]. The results from previous works showed a clear influence of boundary condition on the severity of nonlocal softening effect. In this section, the effect of boundary condition is studied on the vibration response of normalized NI nanobeam model. For this purpose, natural frequencies of FNNI model of nanobeam with different edge conditions are obtained and plotted in Fig. 8 against nonlocal parameter. It is seen in this figure that the natural frequencies decrease as the nonlocal parameter increases for all types of boundary conditions. Further, it is revealed that the nonlocal softening effect intensifies as the edges of nanobeam become more restricted. Moreover, from the figure it is found that the most sensitivity to nonlocal effect is presented by a nanobeam with clamped edges. In fact, as the edges of nanobeam becomes more restricted, the curvature and its variation increases near the edges. Since the strain field in a nanobeam depends on the curvature, and the nonlocal stress also depends on the strain in all points, the severity of nonlocal effect increases for NI beam models with more restricted edges.

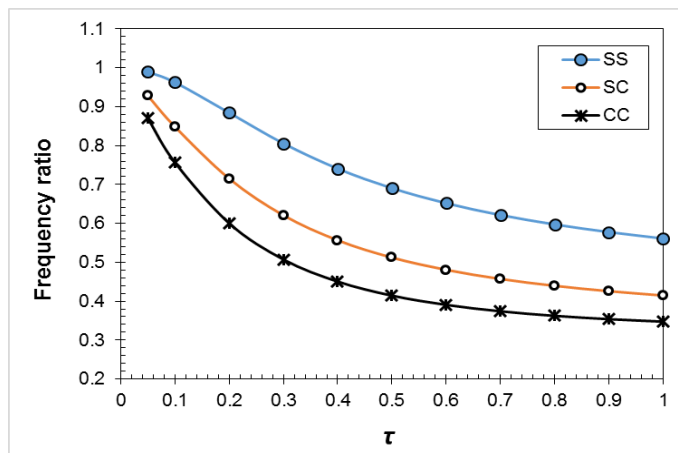


Fig 8 : Effect of boundary conditions on the intensity of nonlocal effect.

4.6. Effect of kernel type

From nonlocal constitutive equation in Eq. (3), it is found that the intensity of nonlocal effect depends on the type of kernel function α . In fact, the kernel function determines the weight of strain at non-adjacent points. Thus, the kernel adjusts the intensity of nonlocal effect imposed on the NI model of nanobeam. To examine the effect of kernel type, frequency ratios for a simply supported FNNI model of nanobeam are plotted against the nonlocal parameter in Fig. 9 for different types of kernel function. It is found from this figure that the small scale effect increases by increasing the nonlocal parameter for all kernels. This arises due to the extension of kernel span by increasing the nonlocal parameter which leads to consideration of strain in more nonlocal or non-adjacent points. Further, from the figure, it is found that the sensitivity of each kernel to nonlocal effect is different and depends severely on the value of nonlocal parameter. For instance, for small nonlocal parameters the exponential kernel is more sensitive to the nonlocal parameter than Gaussian kernel but after a certain value (approximately 0.8) this order becomes reversed. Similar variations are also observed for modified Bessel and triangular kernel functions. The choice of sensitive kernels leads to smaller calibrated nonlocal parameters which are considered to be more logical by some researchers. For example, Wang and Wang [43] reported that the nonlocal parameter e_0a for CNT must be lower than 2 nm. Thus, by choosing an appropriate kernel, one can control the intensity of nonlocal effect imposed on the NI model while maintaining the associated calibrated nonlocal parameter in the admissible range.

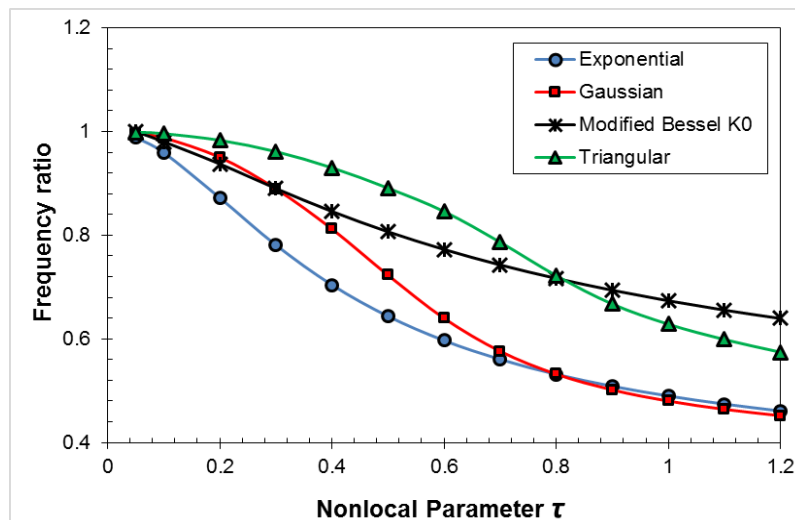


Fig 9 : Effect of different kernel functions on frequency behaviour of TPNI nanobeam model.

4.7. Calibration of NI models according to atomistic models

As mentioned earlier in the introduction section, by calibration of equivalent nonlocal models one can better predict the response of nanostructure. As it was shown in previous sections, the magnitude of frequency of an equivalent continuum model of a nanobeam is severely dependent on the value of nonlocal parameter, particularly, when the normalized kernels are used. The response of NI model is also dependent on the type of kernel as shown in the previous section. Consequently, if the range of admissible nonlocal parameter for a nanostructure is available, a more precise prediction of its dynamic behavior can be made. Further, through calibration process, the behavior of normalized models can be better examined. For calibration process here, a GNR nanostructure is adopted. For most of the calibration process the material with $E=1.01$ Tpa, $\nu=0.16$ and density $\rho=2250$ kg/m³ is adopted unless otherwise stated.

In this section all of the normalized and un-normalized NI models are calibrated using two atomistic models based on AMBER and REBO potentials. These atomistic models have been seen to agree with more precise and expensive simulation techniques such as DFT while are computationally much more efficient [43]. The difference between these two atomistic structural models are in material properties and geometry of bonds which is shown in Fig. 10 and is reported in detail by Shakouri et al. [44]. In these atomistic models of GNR, the carbon atoms are

considered as lumped masses with the mass of 1.9943×10^{-26} kg and the bonds are modeled as beams of the length 0.142 nm. In the AMBER potential, the in-plane stiffness and out-of-plane stiffness of GNR are linked to each other while for the REBO potential field, these two are separated from each other by considering an elliptical cross section for the C-C bond instead of a circular one. It has to be mentioned that all of the atomistic models here are created and analyzed using the ABAQUS software.

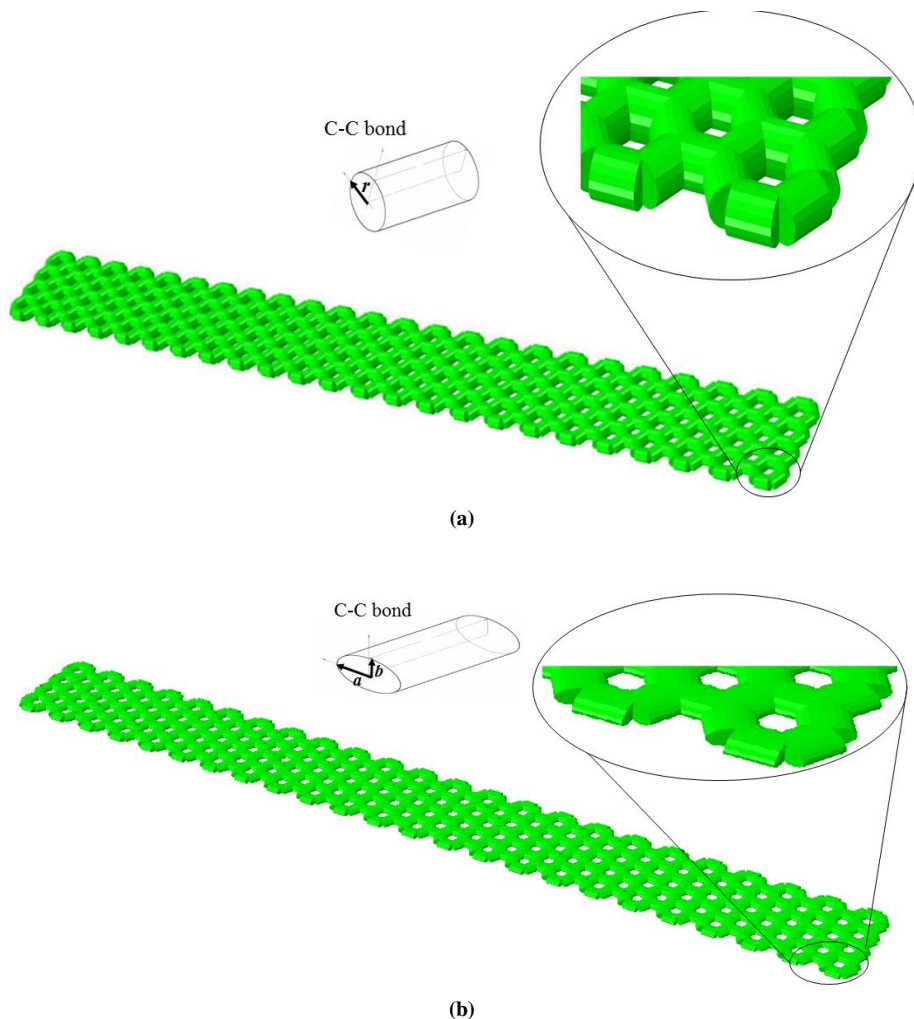


Fig 10: Atomistic model of GNR based on (a) AMBER potential and (b) REBO potential.

At first, the frequencies of NI model with classical exponential kernel function are matched with those from atomistic models. The obtained calibrated nonlocal parameters for the first and second vibration modes are respectively reported in Table 2 and 3 for different sizes, boundary conditions and interatomic potentials (AMBER and REBO). The values in parenthesis are those obtained for REBO potential while the others are for AMBER potential. It is seen in this table that, unlike the nonlocal differential model, as the size of nanobeam increases the value of calibrated nonlocal parameter, τ , remains the same. In fact, if the nonlocal parameter in form of (e_0a) is used here, as used for differential form, the calibrated nonlocal parameter becomes dependent on the size of nanobeam. Thus, it is better to use the non-dimensional form τ for reporting calibrated nonlocal parameters to avoid scattered and confusing results. It has to be noted here that, finding a nonlocal parameter for an equivalent nonlocal continuum model of a nanobeam means that the bending stiffness of its atomistic model is smaller than its corresponding classical continuum model.

It is also found from Table 2 and 3 that as the edges of nanobeam become more restricted (from SS to CC), the value of required calibrated nonlocal parameter decreases. As discussed in Sec. 4.5, this arises due to the increased

nonlocal effect for restricted edges such as clamped edges. In other words, a nanobeam with clamped edge needs lower nonlocal parameter to take the account of nonlocal softening effect and be able to match with atomistic model. Since the CC nanobeam has the highest sensitivity to the nonlocal parameter, as shown in Sec. 4.5, here it needs the lowest calibrated nonlocal parameter in comparison to other boundary conditions. In Fig. 11, the similarity between the first vibration mode of atomistic and equivalent NI model of GNR is presented.

By comparing the results from AMBER potential to those reported in parenthesis for REBO potential in Table 2 and 3, one can find that the atomistic model developed based on the latter potential necessitates higher calibrated nonlocal parameter. This is due to the softer bending stiffness of this atomistic model in comparison to the one developed based on AMBER potential.

The NI nanobeam model is also calibrated in higher vibration modes in Table 3. It is found from the results in this table that similar to the first mode (Table 2), the calibrated nonlocal parameter is independent of length of nanobeam and decreases for stiffer edge constraints. Further, by comparing the results in this table with those in Table 2, it is revealed that for higher vibration modes the value of calibrated nonlocal parameter decreases. As shown in Sec. 4.4, this happens due to severe nonlocal effect in higher modes. So for nanobeam vibrating in higher modes, a smaller nonlocal parameter is required to make the NI model as soft as the atomistic counterpart. Again in this table, it is seen that the values of calibrated nonlocal parameter related to REBO potential are higher than those pertaining to AMBER potential.

The calibration process is also carried out for each normalization scheme in this section and the results are reported for different boundary conditions in Table 4. It is seen in this table that a calibrated nonlocal parameter can be found only for un-normalized and FNNI models and the ANNI model cannot be match with the atomistic model in this case. This is due to specific twofold softening-hardening behaviour of ANNI model which was thoroughly discussed in Sec. 4.2. In fact, for very soft atomistic models a higher nonlocal parameter is required for calibration. However, as it is seen in Fig. 5, the ANNI model shows limited softening and get stiffer after a certain value for the nonlocal parameters. Due to this specific behavior, this model fails to match itself with much softer atomistic model in some cases. Needless to say that this doesn't happen when FNNI model is used for calibration. In fact, this normalized model always shows a monotonic softening behavior as the nonlocal parameter increases.

It also has to be mentioned that even if the ANNI model can be calibrated, there will be two distinct values for the nonlocal parameter [36]. It is now clear that the ANNI model shows inconsistency in calibration process due to its specific twofold behaviour. Such behaviour can lead to confusion and misleading. Thus, it is concluded that not all the normalization schemes are appropriate for dynamic analysis of nanostructures. However, authors suggest the FNNI model for more reliable prediction of nanostructures' response since it doesn't have the above shortcomings.

Table 2: Calibrated nonlocal parameters for NI model of GNR in the first vibration mode for different sizes and boundary conditions (AMBER potential).

<i>L</i> (nm)	<i>b</i> (nm)	Boundary condition			
		SS	CC	CF	SC
10.09	0.98	1.01 (1.40)	0.40 (0.57)	1.07 (1.60)	0.61 (0.86)
7.11	0.98	1.01	0.40	1.08	0.61
4.97	0.98	1.01	0.40	1.08	0.61

Table 3: Calibrated nonlocal parameters for NI model of GNR in the second vibration mode for different sizes and boundary conditions (AMBER potential).

<i>L</i> (nm)	<i>b</i> (nm)	Boundary condition			
		SS	CC	CF	SC
10.09	0.98	0.51 (0.70)	0.30 (0.43)	0.62 (0.88)	0.39 (0.54)
7.11	0.98	0.50	0.30	0.62	0.39
4.97	0.98	0.50	0.31	0.63	0.39

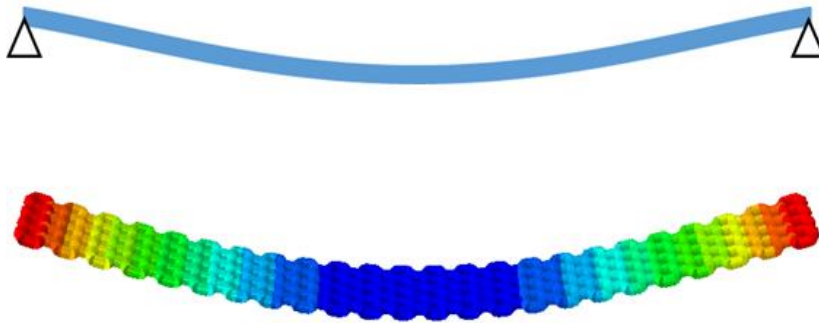


Fig 11 : Similarity of first vibration mode shape of equivalent NI continuum model of GNR (top) to its atomistic model (bottom).

Table 4: Calibrated nonlocal parameter for normalized and un-normalized NI models of GNR based on REBO potential ($L=10.09\text{nm}$, $b=0.98\text{nm}$, $E=2434\text{ Gpa}$, $\nu=0.197$, $\rho=6.316\text{ kg.cm}^{-3}$ [36]).

Model	Boundary condition			
	SS	CC	CF	SC
ANNI	-	-	-	-
FNNI	0.60	0.18	0.74	0.27
Un-normalized	0.39	0.12	0.29	0.19

5. Conclusions

In the present paper, vibration analysis of an equivalent nonlocal integral continuum model of nanobeam has been carried out focusing on the effect of different kernel normalization procedures. In most of the previous studies, this important step either was overlooked or paid not enough attention to. The authors [36] previously showed, for the bending case, that the kernel function must be normalized to avoid violation of natural boundary conditions and excessive softening. Here, the effect of kernel normalization has been studied thoroughly on dynamic behaviour of nanobeam. To this end, an EBT model of nanobeam based on two-phase nonlocal integral model has been developed and its natural frequencies are obtained by the efficient Rayleigh-Ritz method. The kernel function has been normalized via two approaches. To further assess the effect of kernel normalization procedure and other parameters, atomistic models of a typical beam-like nanostructure, here the GNR, are developed to calibrate the equivalent NI model for different sizes, boundary conditions, vibration modes, kernel types and normalization schemes. From the results the following conclusions are drawn:

- The normalization process decreases the intensity of nonlocal softening effect on natural frequencies of nanobeam.
- The two normalized NI models have been seen to predict noticeably different behaviours for vibrating nanobeam.
- One of the normalized models, ANNI model, has been found to show unexpected twofold softening-hardening behaviour with surprising convergence to classical continuum model for large nonlocal parameters.
- It has been found that as the length of nanobeam increases, the intensity of nonlocal effect decreases.
- The nanobeam vibrating in higher modes has been found to be more sensitive to nonlocal effects.
- As the edges of nanobeam becomes more restricted, the nonlocal effects becomes more prominent.
- The intensity of nonlocal effect imposed on the NI model significantly depends on type of kernel function and magnitude of nonlocal parameter.
- It is better to report the calibrated nonlocal parameters in the non-dimensional form τ rather than e_0a to avoid scattered results.
- For a specific nanobeam, the calibrated nonlocal parameter decreases for clamped edges and higher vibration modes.
- The required calibrated nonlocal parameter for a normalized NI model is higher than un-normalized model.
- It has been found that the ANNI model may not be calibrated in some cases due to specific softening-hardening behaviour. Even if this model is able to be calibrated, there will be two separate calibrated nonlocal parameters for this normalized model which will make confusion and paradox.

References

- [1] R. K. Joshi, H. Gomez, F. Alvi, A. Kumar, Graphene films and ribbons for sensing of O₂, and 100 ppm of CO and NO₂ in practical conditions, *The Journal of Physical Chemistry C*, Vol. 114, No. 14, pp. 6610-6613, 2010.
- [2] Q. Liang, J. Dong, Superconducting switch made of graphene–nanoribbon junctions, *Nanotechnology*, Vol. 19, No. 35, pp. 355706, 2008.
- [3] M. Liu, Y.-E. Miao, C. Zhang, W. W. Tjiu, Z. Yang, H. Peng, T. Liu, Hierarchical composites of polyaniline–graphene nanoribbons–carbon nanotubes as electrode materials in all-solid-state supercapacitors, *Nanoscale*, Vol. 5, No. 16, pp. 7312-7320, 2013.
- [4] M. A. Rafiee, W. Lu, A. V. Thomas, A. Zandiatashbar, J. Rafiee, J. M. Tour, N. A. Koratkar, Graphene nanoribbon composites, *ACS nano*, Vol. 4, No. 12, pp. 7415-7420, 2010.
- [5] R. J. Young, I. A. Kinloch, L. Gong, K. S. Novoselov, The mechanics of graphene nanocomposites: a review, *Composites Science and Technology*, Vol. 72, No. 12, pp. 1459-1476, 2012.
- [6] H. Kim, A. A. Abdala, C. W. Macosko, Graphene/polymer nanocomposites, *Macromolecules*, Vol. 43, No. 16, pp. 6515-6530, 2010.
- [7] J. L. Johnson, A. Behnam, S. Pearton, A. Ural, Hydrogen sensing using Pd-functionalized multi-layer graphene nanoribbon networks, *Advanced materials*, Vol. 22, No. 43, pp. 4877-4880, 2010.
- [8] J. W. Kang, S. Lee, Molecular dynamics study on the bending rigidity of graphene nanoribbons, *Computational Materials Science*, Vol. 74, pp. 107-113, 2013.
- [9] R. Faccio, P. A. Denis, H. Pardo, C. Goyenola, A. W. Mombrú, Mechanical properties of graphene nanoribbons, *Journal of Physics: Condensed Matter*, Vol. 21, No. 28, pp. 285304, 2009.
- [10] A. C. Eringen, J. Wegner, Nonlocal continuum field theories, *Appl. Mech. Rev.*, Vol. 56, No. 2, pp. B20-B22, 2003.
- [11] A. C. Eringen, On differential equations of nonlocal elasticity and solutions of screw dislocation and surface waves, *Journal of applied physics*, Vol. 54, No. 9, pp. 4703-4710, 1983.
- [12] J. Reddy, Nonlocal theories for bending, buckling and vibration of beams, *International journal of engineering science*, Vol. 45, No. 2-8, pp. 288-307, 2007.
- [13] A. I. Aria, M. Friswell, A nonlocal finite element model for buckling and vibration of functionally graded nanobeams, *Composites Part B: Engineering*, Vol. 166, pp. 233-246, 2019.
- [14] Ö. Civalek, Ç. Demir, B. Akgöz, Free vibration and bending analyses of cantilever microtubules based on nonlocal continuum model, *Mathematical and Computational Applications*, Vol. 15, No. 2, pp. 289-298, 2010.
- [15] M. Aydogdu, A general nonlocal beam theory: its application to nanobeam bending, buckling and vibration, *Physica E: Low-dimensional Systems and Nanostructures*, Vol. 41, No. 9, pp. 1651-1655, 2009.
- [16] T. Aksencer, M. Aydogdu, Levy type solution method for vibration and buckling of nanoplates using nonlocal elasticity theory, *Physica E: Low-dimensional Systems and Nanostructures*, Vol. 43, No. 4, pp. 954-959, 2011.
- [17] W. Duan, C. M. Wang, Exact solutions for axisymmetric bending of micro/nanoscale circular plates based on nonlocal plate theory, *Nanotechnology*, Vol. 18, No. 38, pp. 385704, 2007.
- [18] T. Murmu, S. Pradhan, Small-scale effect on the free in-plane vibration of nanoplates by nonlocal continuum model, *Physica E: Low-dimensional Systems and Nanostructures*, Vol. 41, No. 8, pp. 1628-1633, 2009.
- [19] T. Murmu, J. Sienz, S. Adhikari, C. Arnold, Nonlocal buckling of double-nanoplate-systems under biaxial compression, *Composites Part B: Engineering*, Vol. 44, No. 1, pp. 84-94, 2013.
- [20] R. Ansari, S. Sahmani, B. Arash, Nonlocal plate model for free vibrations of single-layered graphene sheets, *Physics Letters A*, Vol. 375, No. 1, pp. 53-62, 2010.
- [21] R. Li, G. A. Kardomateas, Vibration characteristics of multiwalled carbon nanotubes embedded in elastic media by a nonlocal elastic shell model, 2007.
- [22] F. Khademolhosseini, R. Rajapakse, A. Nojeh, Torsional buckling of carbon nanotubes based on nonlocal elasticity shell models, *Computational materials science*, Vol. 48, No. 4, pp. 736-742, 2010.
- [23] J. Peddieson, G. R. Buchanan, R. P. McNitt, Application of nonlocal continuum models to nanotechnology, *International journal of engineering science*, Vol. 41, No. 3-5, pp. 305-312, 2003.
- [24] H. Ersoy, K. Mercan, Ö. Civalek, Frequencies of FGM shells and annular plates by the methods of discrete singular convolution and differential quadrature methods, *Composite Structures*, Vol. 183, pp. 7-20, 2018.

- [25] Ö. Civalek, Ç. Demir, Bending analysis of microtubules using nonlocal Euler–Bernoulli beam theory, *Applied Mathematical Modelling*, Vol. 35, No. 5, pp. 2053-2067, 2011.
- [26] S. Shaw, P. Murthy, S. Pradhan, The effect of body acceleration on two dimensional flow of Casson fluid through an artery with asymmetric stenosis, *The Open Conservation Biology Journal*, Vol. 2, No. 1, 2010.
- [27] J. Fernández-Sáez, R. Zaera, J. Loya, J. Reddy, Bending of Euler–Bernoulli beams using Eringen’s integral formulation: a paradox resolved, *International Journal of Engineering Science*, Vol. 99, pp. 107-116, 2016.
- [28] C. Li, L. Yao, W. Chen, S. Li, Comments on nonlocal effects in nano-cantilever beams, *International Journal of Engineering Science*, Vol. 87, pp. 47-57, 2015.
- [29] M. Tuna, M. Kirca, Exact solution of Eringen's nonlocal integral model for bending of Euler–Bernoulli and Timoshenko beams, *International Journal of Engineering Science*, Vol. 105, pp. 80-92, 2016.
- [30] M. Tuna, M. Kirca, Exact solution of Eringen's nonlocal integral model for vibration and buckling of Euler–Bernoulli beam, *International Journal of Engineering Science*, Vol. 107, pp. 54-67, 2016.
- [31] Y. Wang, X. Zhu, H. Dai, Exact solutions for the static bending of Euler–Bernoulli beams using Eringen’s two-phase local/nonlocal model, *Aip Advances*, Vol. 6, No. 8, pp. 085114, 2016.
- [32] J. Fernández-Sáez, R. Zaera, Vibrations of Bernoulli-Euler beams using the two-phase nonlocal elasticity theory, *International Journal of Engineering Science*, Vol. 119, pp. 232-248, 2017.
- [33] X. Zhu, Y. Wang, H.-H. Dai, Buckling analysis of Euler–Bernoulli beams using Eringen’s two-phase nonlocal model, *International Journal of Engineering Science*, Vol. 116, pp. 130-140, 2017.
- [34] K. Eptaimeros, C. C. Koutsoumaris, G. Tsamasphyros, Nonlocal integral approach to the dynamical response of nanobeams, *International Journal of Mechanical Sciences*, Vol. 115, pp. 68-80, 2016.
- [35] K. Eptaimeros, C. C. Koutsoumaris, I. Dernikas, T. Zisis, Dynamical response of an embedded nanobeam by using nonlocal integral stress models, *Composites Part B: Engineering*, Vol. 150, pp. 255-268, 2018.
- [36] A. Anjomshoae, B. Hassani, On the importance of proper kernel normalization procedure in nonlocal integral continuum modeling of nanobeams, *ZAMM-Journal of Applied Mathematics and Mechanics/Zeitschrift für Angewandte Mathematik und Mechanik*, Vol. 101, No. 10, pp. e202000126, 2021.
- [37] L. Shen, H.-S. Shen, C.-L. Zhang, Nonlocal plate model for nonlinear vibration of single layer graphene sheets in thermal environments, *Computational Materials Science*, Vol. 48, No. 3, pp. 680-685, 2010.
- [38] A. Shakouri, T. Ng, R. Lin, A study of the scale effects on the flexural vibration of graphene sheets using REBO potential based atomistic structural and nonlocal couple stress thin plate models, *Physica E: Low-dimensional Systems and Nanostructures*, Vol. 50, pp. 22-28, 2013.
- [39] S. B. Altan, Uniqueness of initial-boundary value problems in nonlocal elasticity, *International journal of solids and structures*, Vol. 25, No. 11, pp. 1271-1278, 1989.
- [40] G. Borino, B. Failla, F. Parrinello, A symmetric nonlocal damage theory, *International Journal of Solids and Structures*, Vol. 40, No. 13-14, pp. 3621-3645, 2003.
- [41] Z. P. Bažant, M. Jirásek, Nonlocal integral formulations of plasticity and damage: survey of progress, *Journal of engineering mechanics*, Vol. 128, No. 11, pp. 1119-1149, 2002.
- [42] S. Chakraverty, L. Behera, Free vibration of non-uniform nanobeams using Rayleigh–Ritz method, *Physica E: Low-dimensional Systems and Nanostructures*, Vol. 67, pp. 38-46, 2015.
- [43] Q. Wang, C. Wang, The constitutive relation and small scale parameter of nonlocal continuum mechanics for modelling carbon nanotubes, *Nanotechnology*, Vol. 18, No. 7, pp. 075702, 2007.
- [44] A. Shakouri, T. Ng, R. Lin, A new REBO potential based atomistic structural model for graphene sheets, *Nanotechnology*, Vol. 22, No. 29, pp. 295711, 2011.